IChemE

0263–8762/00/$10.00+0.00

Trans IChemE, Vol 78, Part A, September 2000

MODELLING TRANSPORT PHENOMENA AND PERFORMANCE OF DIRECT METHANOL FUEL CELL STACKS

K. SCOTT (FELLOW), P. ARGYROPOULOS and W. M. TAAMA

Department of Chemical and Process Engineering, University of Newcastle upon Tyne, Newcastle upon Tyne, UK

A prototype direct methanol fuel cell (DMFC) stack has been designed and built at Newcastle University, based on a flow bed design developed with the aid of a flow visualization study and fluid flow modelling. In addition, a series of engineering models have been developed that predict the stack voltage, fluid distribution from the stack manifolds, the overall system pressure, the chemical equilibrium in both anode and cathode flow beds and the thermal management of the stack. The results of this work are presented in terms of an overall engineering model that incorporates all the aforementioned models. The initial steady state performance data of the prototype stack presented was obtained as a result of our experience of scaling up the system to achieve the designed power outputs.

Keywords: fuel cell; direct methanol; solid polymer electrolyte stack; modelling

INTRODUCTION

A polymer eletrolyte fuel cell stack consists of a number of single cells connected electrically in series. Typically the stack is composed of several components:

- Two end plates, which are used to align and compress the stack, two insulation sheets which isolate the end plates from current collector plates;
- Membrane electrode assemblies (MEA) consisting of two catalyst layers, one as cathode the other as anode, attached to the polymer electrolyte membrane (PEM), which serves both as cell separator and electrolyte. Two carbon-backing layers serve as support for uncatalysed gas diffusion layers and for the catalyst layer in each;
- Bipolar plates, for fuel and oxidant flow, which have flow channels on both surfaces and are in electrical contact with the MEA.

The membrane electrode assemblies are sandwiched between the bipolar plates. The MEA is electrically insulated at its sides to avoid a cell short-circuit. This insulation material (e.g. Teflon), also serves as a seal for the cell. The repeated section of bipolar plate/flow channels and MEA constitutes the fuel cell stack. The last two graphite plates in the stack are different to the bipolar plates, as they have channels machined on only one side, the other side is in direct contact with the current collector. Figure 1 shows a schematic representation of the DMFC.

The liquid feed direct methanol fuel cell (DMFC), based on a solid polymer electrolyte (SPE), is seen as a potential power source in static and transport applications, due to its inherent simplicity of operation, e.g. conversion of a dilute aqueous based fuel into a gaseous product. Currently significant power performance has been achieved with the use of catalysts based on Pt-Ru[1–10]. Typically, power densities higher than 0.18 W cm^{-2} have been achieved, and power densities higher than 0.3 W cm^{-2} have been reported[3]. For high performance of a DMFC relatively low concentrations of methanol are required. At concentrations higher than approximately 2 mol dm^{-3}, the cell voltage declines significantly due to permeation of methanol through the membrane, i.e. methanol crossover. This permeation results in a mixed potential at the cathode, with a significant loss in oxygen reduction performance, and also poor fuel utilization. As the development work continues, the engineering research of the system becomes more significant as commercialization of the relative technology becomes more realistic. Research of direct methanol fuel cells (DMFC) based on solid polymer electrolyte (SPE) has mainly been in steady state and small-scale operations within laboratory environments. The construction of a successful DMFC stack will require identification and realization of the proper solution of the major problems likely to be encountered in large-scale systems. Such problems are:

- The continued need for anode and cathode side improvements in terms of materials, design and performance;
- Minimizing methanol crossover through the membrane;
- Maintain a proper water balance especially in the cathode side compartment to avoid solid polymer electrolyte dehydration, thus increasing its resistance and lowering the performance achieved;
- The heat loss/gain within every cell arising from the intrinsic conversion efficiency of methanol to electricity and also to minimize the necessary heat loads required for cold start-up;
- The design of the stack system with minimum possible complexity and low thermal and hydraulic inertia, thus maintaining the ability for fast response under variable load conditions;

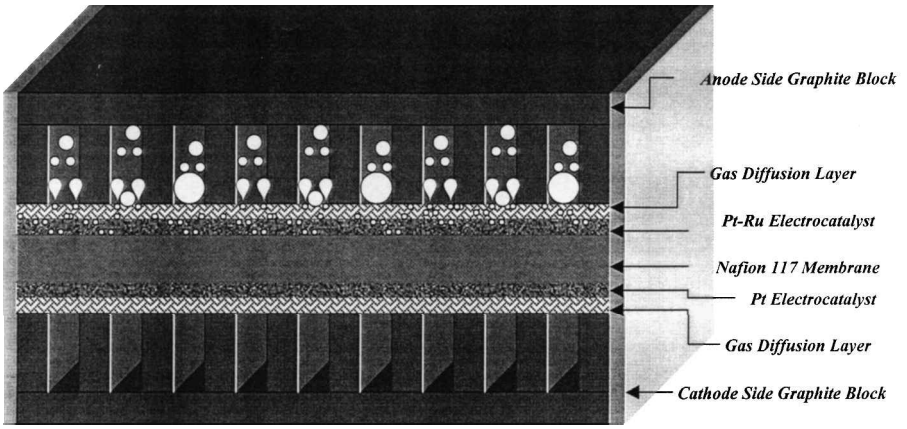

Figure 1. Schematic representation of a DMFC. Anode: $CH_3OH + H_2O \Rightarrow CO_2 + 6H^+ + 6e^-$. Cathode: $\frac{3}{2}O_2 + 6H^+ + 6e^- \Rightarrow 3H_2O$. Overall: $CH_3OH + \frac{3}{2}O_2 \Rightarrow CO_2 + 2H_2O$.

• The control of the exhaust gases which contain methanol vapour, a fact which also poses a significant design requirement for fuel management;
• Simple design, with low cost, environmental friendly, commercially available materials, reliable sealing between the cells and minimum catalyst loading with high utilization.

In the following sections the progress made in Newcastle is reported in these key areas for system development. Performance data for a 3-cell stack system used to commission the system is also reported.

CELL STACK DESIGN, CONTROL AND OPERATING SYSTEM

A prototype DMFC stack and system was designed and built based on a series of bipolar connected MEAs each with active areas of 272 cm^2. The stack consists of the following components:

i. Two stainless steel end plates, which are used to align and compress the stack,
ii. two polypropylene sheets which isolate the end plates from the stainless steel current collector plates, and 25 mm thick nuclear grade Poco® graphite flow bed end plates, and
iii. membrane electrode assemblies (MEA).

The MEAs are fabricated from two carbon-backing layers as support for the uncatalysed gas diffusion layers and for the catalyst layer on each side of the solid polymer electrolyte, Nafion® 117 (Du Pont de Nemours). Preparation procedures for the MEA have been described elsewhere[11]. Non porous heat transfer grade Poco® graphite of 8 mm thickness, acts as bipolar plates, and for fuel and oxidant flow. These have flow channels machined on both surfaces and are in electrical contact with the carbon backing layer. The cell stack is internally manifolded for the separate flow of air and methanol solution. The air and liquid flow connections are to one of the graphite flow bed end plates to enable the use of any number of cells, from 1 to 25, without disturbing the flow circuit configuration. The cell flow circuit, shown in Figure 2a, provides a controlled rate of fuel and oxidant flow.

Electrical/electronic control of the stack is through the output of the cell with switched-mode power electronics, and mimics the load with a second power electronic converter. The second converter acts as a programmable load to allow various dynamic load situations to be examined. The overall process is controlled using a micro-controller, with the power conditioning and programmable load controlled by their own micro-controllers. A PC is used as the software platform for the system. Individual cell voltages can be monitored using a multiplexer unit. Methanol fuel concentration is controlled through a PC based model of methanol consumption. The model predicts the total methanol consumption: at the anode, methanol crossover and vaporization after the condensers. Methanol is added to the methanol solution feed tank, from a methanol reservoir, using a separate peristaltic pump. The control was supported by regular off-line measurement of methanol concentration. The cathode side exhaust gas passes through a glass condenser, and the condensate is collected in a small tank. A third Watson-Marlow 505S peristaltic pump returns the collected condensate from the cathode side outlet manifold, to the water-methanol tank so as to avoid supplying water for replenishing the quantity lost. All the exhaust side tubing was made from 25 mm ID glass and the supply loops were made from 15 mm ID S316 stainless steel tubing. Coolers, storage and collection tanks were all glass (30 dm^3 for the solution tank, 12 dm^3 for the cathode side condensate collection tank) and were airtight. The circulation of methanol was by a parallel connection of two centrifugal magnetically driven Totton pumps with PVDF heads. The anode side exhaust passed through a specially designed separation tank. The liquid flows downwards to the main reservoir where residual gas is vented from the top of the column through a glass condenser, to recover vaporized methanol from the carbon dioxide gas exhaust. A set of two Platon Fmet series flow meters with two precision valves is used to control the air supply. The cathode side exhaust gas is passed through a collection tank, to trap the water separated from the air with the aid of a second condenser placed on the top of the vessel. For cold start-up, the necessary heat is provided to the cell stack with a pair of in house produced heating plates with embedded resistances. The cell stack temperature can be controlled using PC based control of the power source to the resistors, a Farnel AR60-50 regulated power supply source.

The necessary heat load for the stack start-up and for

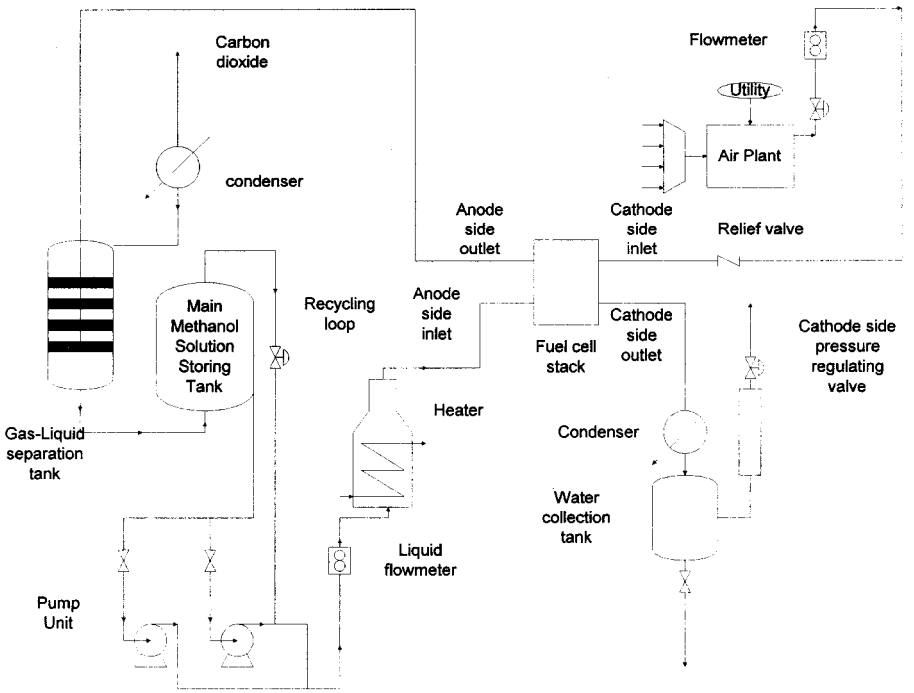

(a)

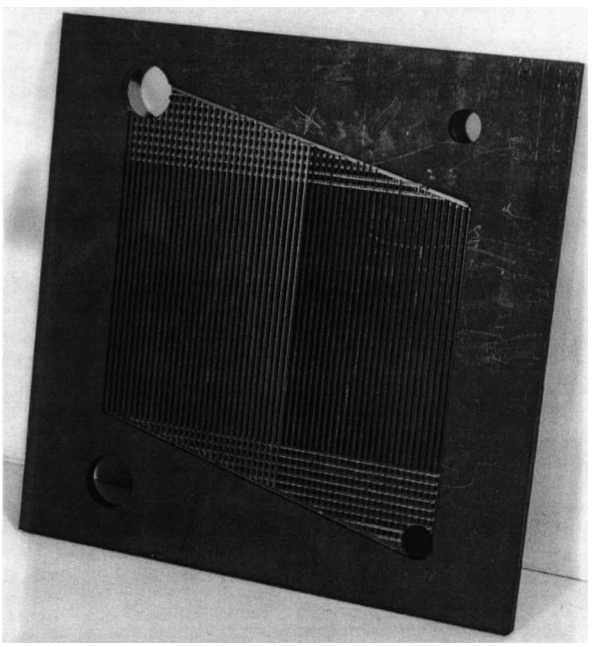

(b)

Figure 2. Schematic representation of the prototype stack testing facility and the flow bed design. (a) Experimental flow circuit. (b) Bipolar plate design.

replenishing the heat losses was provided, to the methanol solution stream by a Watlow 1.25 kW stainless steel heater, controlled by an embedded thermocouple and an external PID temperature controller. For large-scale operation, a compressor supplied air at the required pressure and flow rates. A dust and oil filter is installed at the compressor's outlet to prevent contamination of the MEA. A humidifier and an air heater are not vital for stack operation with liquid feed, since there is sufficient humidity available at the cathode side and no membrane dehydration problems were detected. The flow beds are based on the design (Figure 2b) developed from the flow visualization study[12,13].

Experimental cell voltage and current density data were collected when steady state was apparently achieved. The data are the average of three repeated runs performed by polarizing the stack with increasing load and then with decreasing load.

ENGINEERING ISSUES OF LARGE SCALE CELL STACKS

The good steady-state performance of a bipolar fuel cell stack is dependent upon several factors including:

- Achieving uniform distribution of flow between the cells and within each individual cell to avoid localized fuel or oxidant starvation;
- Achieving a uniform distribution of current and potential over the surface of each electrode and throughout the cell structure;
- Efficient heat removal from the surface of the electrodes and the membrane to avoid excessive temperature variations;
- Adequate hydration of the membrane over the complete surface to maintain membrane stability;
- Minimizing pressure losses to reduce the energy consumption of the pumps and compressors;

Thermal management is a concern in every SPE fuel cell design due to the sensitive nature of the electrochemical process, the compact cell stack design and the restrictive geometry limitations. In general, the stack system is characterized by a large thermal inertia. Although approaching a thermal steady state condition is feasible in a moderate time interval (less than 30 min for large stacks), the achievement of a real steady state situation may take a few hours. The stack temperature is strongly affected by the surroundings temperature, the presence of a thermal insulation and the use of heating plates. The heating plates have a function in the stack system, to help to minimize the time interval required for the stack to be heated to the required temperature (see Figure 3). Experience has shown that for small stacks of less than five cells, in an un-insulated system, the stack temperature could not be increased above 80°C except if heating plates are used. Nevertheless on moving towards stack operation with a large number of cells, the role of the heating plates is minimized. The membrane material is not a good heat conductor posing a significant barrier for heat to be transferred between the cells. In addition, the successive cathode sides reduce the ability for heat transfer to the membrane electrode assemblies, either by their low, in plane, thermal conductivity or by simply removing the heat away from the stack body.

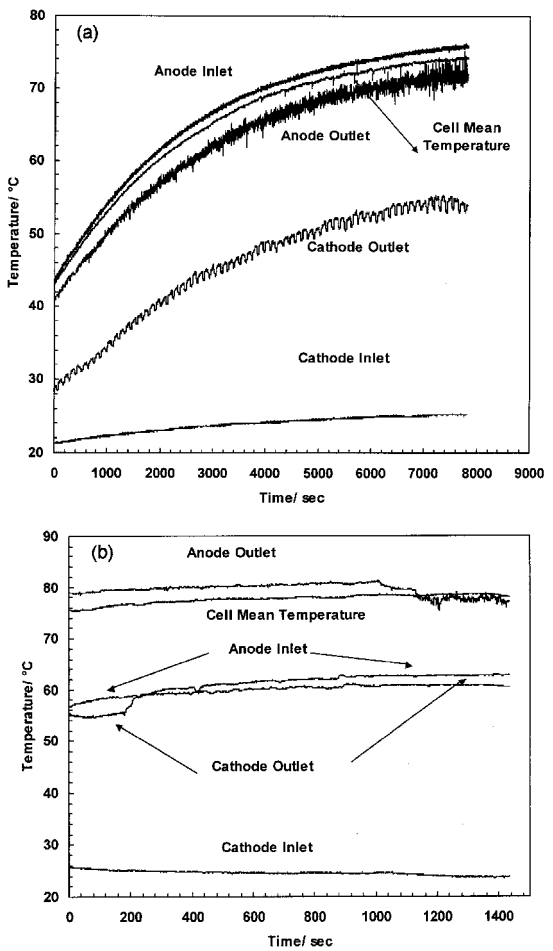

Figure 3. Demonstration of the 3-cell stack system thermal inertia for: (a) preheated feed only operation (b) Combined preheated feed and stack operation, 50 mA cm^{-2}, 1.2 V average stack voltage. 1.0 M methanol solution at a flow rate of 5.5 dm^3 min^{-1}, 1.7 bar air pressure.

Figure 3 shows the typical temperature transients for the three cell stack system without a current load and when the methanol solution alone is heated. It takes approximately one hour for the system to approach the steady state temperature of operation, of approximately 70°C (Figure 3a). There is approximately 2°C difference in the anode side inlet and outlet temperatures, the cathode exhaust temperature reaches approximately 56°C. Clearly the system response shown in Figure 3a is specific to the stack and the volume of methanol solution, but is indicative of the relatively slow start up of the stack without parasitic heat generation for the stack itself on load. The response is a measure of the relatively poor heat transfer between the methanol solution and the cell stack, especially when ambient pressure air is used which further serves to cool the cell. The requirements for good insulation are clear, although in practice this partly conflicts with the requirements of heat release during operation, where control of stack body temperature may be achieved by convective and radiative heat transfer.

Figure 3b shows the temperature responses of the cell stack system when a load of 50 mA cm^{-2} is applied, after the start up period, as shown in Figure 3a. The cell temperature rises by approximately 2°C over the first 400 seconds and then remains approximately constant. This indicates that although steady state temperatures can be maintained, the system itself shows significant thermal inertia when current loads are applied or changed.

Pressure losses in the cell stack are directly related to manifold and flow bed design and, to a smaller extent, the stack thermal management. Two areas of stack design are of interest in the case of pressure losses:

1. for the anode side, where the pressure losses are to be kept low to minimize the pump size and cost, and,
2. for the cathode side where if the pressure loss is small then an expensive and energy consuming compressor can be replaced by an air blower with lower energy demand.

Figure 4a shows pressure drop measurements for an increasing number of stacked cells as a function of anode side inlet flow rate in the range of 1.0 to 6.0 dm^3 min^{-1}. Essentially these are representative values for the hydraulic

resistance of the system at 60°C without air flowing at the cathode, i.e. there was no electrochemical activity and the measurements were slightly biased in the sense that the membrane electrode assemblies were pushed against the cathode side flow beds, thus reducing the actual pressure drop. As can be seen from Figure 4a, as the total openings cross-sectional area exceeds the inlet manifold area, i.e. as the number of cells increases, the pressure drop falls rapidly. In addition, for a large number of cells, and with low flow rates, there is a limited practical effect of the cell number on the pressure drop, due to the laminar flow conditions and also to the beneficial effect of the sucking (outlet) manifold, whose influence increases with its length and number of openings (i.e. cell ports). Similar data is shown in Figure 4b for a 10-cell stack with air supplied at room temperature to the cathode side. As can be seen, the changes in the pressure head are quite low not justifying the use of a compressor for air supply in the system, at least to overcome the pressure losses in the cell stack.

STACK ELECTRICAL PERFORMANCE

The performance of a 3-cell stack system was studied as the commissioning phase of the DMFC system. Prior to performance testing, the stack is conditioned following procedures described elsewhere for small-scale cells[1]. Two different modes of operation were used: combined pre-heated stack and feed supplied to the cell, with a pressurized air fed cathode, and operation with preheated feed only with uncompressed air supply. Immediately after the condition phase, and after adding methanol to the anode feed, the stack voltage rose to values comparable with the small cells, and upon preliminary testing the cells delivered performances only 5–10% lower than the small cells (i.e. 1.8 V at open circuit, 0.9 V at 50 mA cm^{-2} at a temperature of 70°C). This was achieved with the cell and liquid methanol solution both heated. In practice the cell stack would not be heated separately, and thus data was collected with only preheated liquid. Data is presented as the measured total voltage divided by the open circuit voltage to enable comparison with small scale cell data.

Preheated feed tests were performed to assess the feasibility of operating a large scale fuel cell stack with only preheated feed, and to identify issues associated with this mode of operation that can be the subject of future research. Figure 5 shows the effect of anode side inlet flow rate on the stack output voltage, for a 3-cell stack being operated with 1.0 M preheated methanol solution at 70°C the stack mean temperature is 70°C, and the cathode supply was 15 $dm^3\,min^{-1}$ of low pressure air (0.1 bar). The data are in general agreement with that expected from small cell testing and the modelling work. The differences in the stack response, due to the increase in the flow rate, can be explained from the heat transfer characteristics of the system. At the lower flow rate, the residence time in the anode side flow bed is higher, and hence the liquid is heated to higher temperatures close to those of the stack body. On the contrary, when large flow rates are used, despite the higher heat transfer coefficients achieved, the short residence time does not allow for sufficient liquid heating. Hence the liquid enters the catalyst layers at a lower temperature (5 K less) than the stack body, thus cooling the catalyst layers and, accordingly, the performance of the

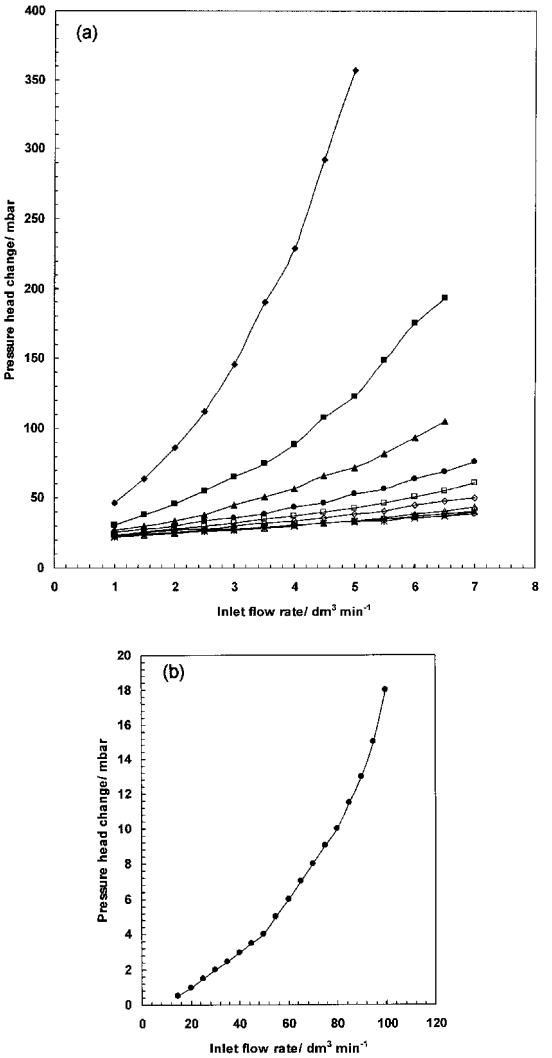

Figure 4. Anode and cathode side pressure head variation measurements as a function of increasing anode/cathode side inlet flow rates for a range of stacked cells ◆1 ■2 ▲3 ●4 □5 ◇6 △7 ✳8 ×9 ○ 10.

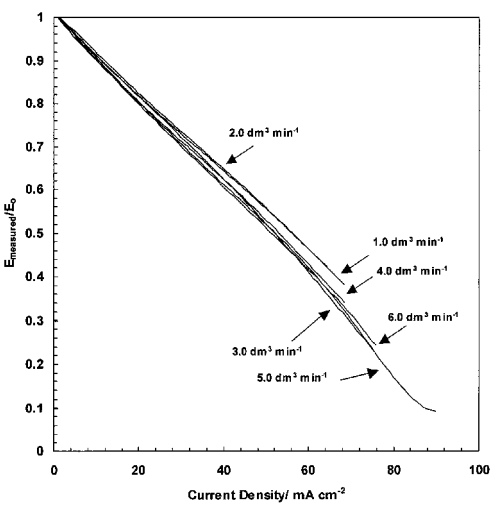

Figure 5. 3-cell stack voltage output as a function of increasing methanol solution inlet flow rate in $dm^3\,min^{-1}$ (1.0 M preheated methanol solution at 70°C, stack mean temperature 70°C, 15 $dm^3\,min^{-1}$ unpressurized air supply).

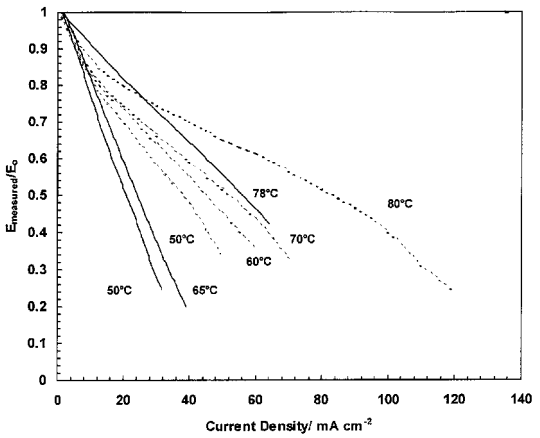

Figure 6. Comparison of the effect of feed inlet temperature on the electrical response of the 3-cells stack and the small cell both being operated at the preheated feed mode with 1.0 M aqueous methanol solution 70°C, and 0.3 bar cathode side pressure (----: small cell, ——: large scale 3 cell stack).

anodic endothermic reaction is reduced. The detrimental effect of higher flow rates on the voltage due to heat transfer limitations is, however, partly affected by the expected advantages in gas bubble management and mass transport.

Figure 6 compares the effect of temperature on voltage response for the 3-cell stack and a small-scale cell with similar operating conditions. A difference between the two systems for the small-scale cell is that the feed is preheated using a constant temperature bath, which minimizes the feed temperature variations with the increase of the flow rate. Hence, an increase in the feed supply flow rate can lead to an increased heat supply in the cell, which in turn can increase its performance. As can be seen, the electrical output from both the cell stack and the small cell are not radically different. Except for the absence of the activation region for the stack, the two systems respond similarly with the stack output being slightly higher, with higher temperatures giving higher voltages. At low temperatures of 50 to 60°C, the stack performance is significantly lower than the small-scale cell. In the case of the stack, the temperatures at the catalyst layers are expected to be significantly lower than the measured stack body temperature. It is known from small scale cell tests at low temperatures (< 50°C), that a few degrees variation in temperature causes a significant variation in power voltage output due to the sluggish nature of anodic methanol oxidation. At temperatures of 70°C and above the stack performance and the small scale cell performances are comparable.

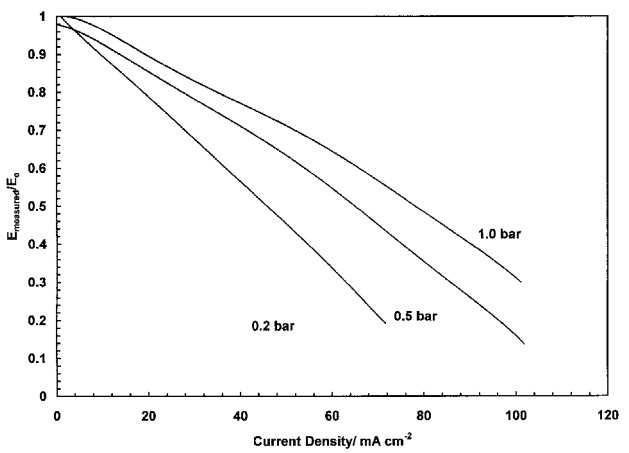

Figure 7. 3-cell stack voltage output as a function of increasing cathode side overpressure (1.0 M preheated methanol solution supplied at 1.5 dm^3 min^{-1} at 75 °C, stack mean temperature 80°C, 15 dm^3 min^{-1} air supply).

Figure 7 shows the effect of an increase in cathode side air pressure on stack performance. A modest improvement in performance is achieved, e.g. at approximately half the open circuit cell voltage ($E/E_o = 0.5$) there is almost a doubling in the current density output (e.g. from 48 mA cm^{-2} to 88 mA cm^{-2}). This response to an air pressure increase is markedly different to that observed in small-scale cells. In addition, the open circuit potential increased by 40 mV per cell in the stack on increasing the air pressure from 0.2 bar to 1.0 bar. Although an increase in air pressure can benefit the cathode reaction by increasing the partial pressure of oxygen, an additional factor is that higher air pressures also reduce the crossover of methanol from the anode side. This reduces the extent of cathode depolarization with a noticeable performance improvement, which is maintained over the full range of current outputs.

It should be noted that, with this mode of operation, a temperature higher than 75°C could not be achieved due to the limited heater capacity and the large capacity of the methanol storage tank, which lead to significant heat losses to the surroundings. The large exposed areas of the external loop meant that the liquid was maintained at temperatures just above 50–55°C.

MODELLING OF DIRECT METHANOL FUEL CELL STACKS

A large number of issues arise from scaling up single small scale DMFCs; flow distribution from the stack manifolds, thermal management, pumping requirements, exhaust gases and liquid feed that has to be circulated, heated, and carbon dioxide disengagement. The exact nature and magnitude of these processes, and their effect on a large multi cell stack, has only recently been addressed in a systematic way with the aid of mathematical modelling and experimental studies[4–11]. These preliminary modelling studies were developed to aid the design of the prototype stack system. A number of limitations existed in the models; for instance the thermal model[8,9] was based on a different flow bed design, of 57 parallel channels, to that used here, and the flow bed temperature profiles for the other models[4,5,7,10,11] were based on a linear formulation between the inlet and the outlet port. Essentially every one of the models was discrete, relying on user inputs that describe the three remaining aspects, that in most cases were simplifying assumptions, such as equal flow distribution, isothermal operation, absence of vapour-liquid equilibrium, frictionless flow, etc. In other cases, simplifications concerning the use of single-phase behaviour for equations and correlations were used to describe pressure drop terms and heat transfer processes. To some extent complex aspects, such as the flow bed spots areas, the liquid phase vaporization in the case of the hydraulic models, the flow and heat transfer processes in both cell manifolds and in the spots area, and the effect of thermal and fluid distribution on the systems physical properties were omitted.

DMFC stacks are still being used in elevated temperatures above the solution boiling point (85–90°C depending on pressure and methanol concentration), and hence localized boiling occurs within the anode side flow beds. Subcooled liquid heat transfer and nucleate boiling differ a lot from conventional convective heat transfer. For the flow bed design developed by the authors, geometry plays an important role, as the flow characteristics vary significantly along the flow bed length. A serious revision of the critical aspect of flow bed heat transfer theoretical treatment was, therefore, deemed necessary to increase the model accuracy. In the present model development, which was initiated after the design of the stack system, a more detailed study was undertaken in an effort to remove as many as possible of these simplifying assumptions[12].

The new model formulation is extended to accommodate new characteristics such as:

- Spots area pressure drops and heat transfer characteristics have been included;
- Two-phase flow, boiling and nucleate heat transfer correlations are used for the calculation of the local heat transfer coefficients;
- Two-phase flow correlations have been used for all aspects of the hydraulic models;
- Vapour-liquid equilibrium calculations have been carried out for the entire stack length;
- Heat transfer and flow mixing model have been included for the stack manifolds.

Figures 8–11 show typical results produced from the model for the case of a 3-cell stack. Figure 8 shows the effect of an increase in anode side inlet flow rate on the predicted stack longitudinal profile. The major impact of a change in flow rate is to modify the fraction of gas produced in the methanol solution which affects local hydrodynamics, pressure and heat transfer. Depending upon the local cell conditions, the heat transfer coefficient can either decrease or increase with flow rate due to variations in two phase flow and boiling heat transfer. As can be seen, the overall stack temperature gradient between the two current collectors increases as the anode side inlet flow rate increases. At high

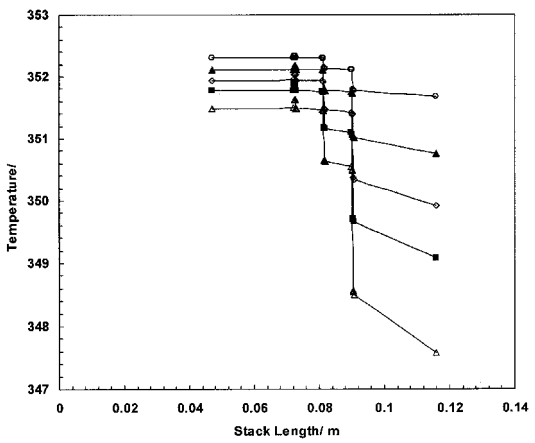

Figure 8. Model predicted longitudinal stack temperature profile between the two current collectors as a function of increasing anode side inlet flow rate at the range 0.5–3 $dm^3 min^{-1}$ for a 3 cell stack operated at a current density of 100 mA cm^{-2} with 1.0 M aqueous methanol solution at 351 K and 5 $dm^3 min^{-1}$ ambient pressure air supply at 293 K. ⊸ 0.5 dm^3/min; ▲ 1.0 dm^3/min; ◇ 1.5 dm^3/min; ■ 2.0 dm^3/min; △ 3.0 dm^3/min.

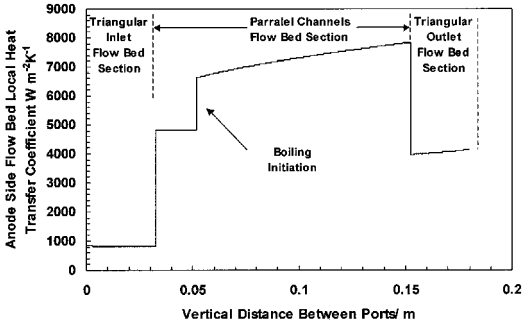

Figure 9. Middle cell predicted local anode side flow bed heat transfer for a 3 cell stack operated with a current density 100 mA cm^{-2} at an anode side inlet flow rate of 1.5 $dm^3 min^{-1}$ of 1.0 M aqueous methanol solution at 80°C and 5.0 $dm^3 min^{-1}$ ambient pressure air supply at 293 K.

flow rates this temperature difference is approximately 2 K, which indicates that a modest variation in cell performance could result for a low number of three cells in the stack. This can be explained from the critical role of the solid polymer electrolyte which restricts the ability to transfer heat from the anode side to the cathode side of each cell, and in addition, restricts the amount of excess heat that can be transferred from one cell to the other through the bipolar plates. Hence, as flow rate decreases the amount of excess heat transferred to every cell falls and there is movement towards an isothermal operation.

Figure 9 shows the effect of two-phase flow and boiling initiation on the values of the local anode side heat transfer coefficients for the middle cell of the stack. As can be seen, boiling heat transfer is more intense than that for two phase, thus improving heat transfer to the anode side electrocatalyst layer. This variation in heat transfer coefficient has immediate implication on the stack thermal, and hydraulic and power response.

Figure 10 shows the effect of boiling initiation on the anode flow bed temperature profile in the mid stacked cell at different values of current density. The temperature change from inlet to exit is just less than 1.0°C at all current densities, although the temperature profile changes with current density. This is due to the influence of an increased volume of gas at higher current densities and the different point of initiation of boiling, which changes the slope of the temperature decrease with increasing flow bed length.

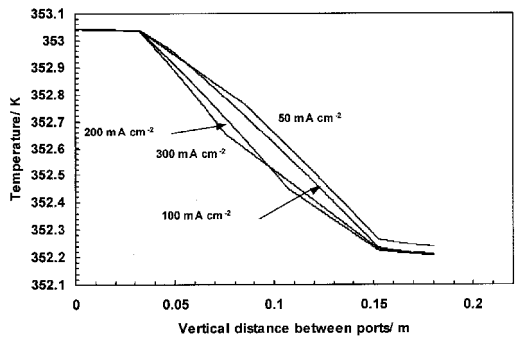

Figure 10. Model predicted temperature profile across the middle stacked cell cathode side flow bed as a function of increasing current density at the range 50–300 mA cm^{-2}, for a 3 cell stack operated at an anode side inlet flow rate of 1.5 $dm^3 min^{-1}$ of 1.0 M aqueous methanol solution at 80°C and 5.0 $dm^3 min^{-1}$ ambient pressure air supply at 293 K.

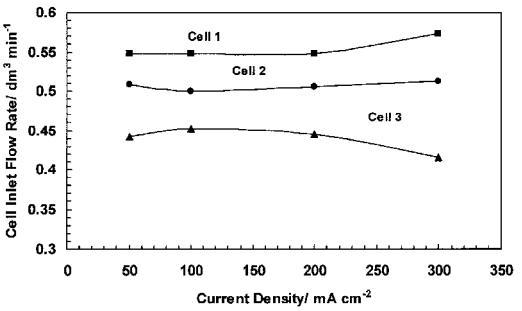

Figure 11. Anode side flow distribution patterns for a 3-cell stack as a function of increasing current density (1.0 M aqueous methanol solution, supplied at a flow rate 1.5 $dm^3\,min^{-1}$ and preheated at 80°C, cathode side flow rate 5.0 $dm^3\,min^{-1}$ of unpressurised air supplied at 20°C).

Figure 11 shows a sample prediction for the effect of an increase in current density on the flow distribution pattern of the anode side of a 3-cell stack. It is evident that the increase in carbon dioxide generated from the electrochemical reaction, and the changes in the vapour-liquid equilibrium point, affect the flow distribution within the stacked cells. Even with a 3 cell stack the variation in flow between the cells is significant, e.g. approximately 20%, and increases with an increase in current density. It is thus expected that with a greater number of cells the flow distribution will be even less uniform, leading to potential operating problems with the stack in terms of uniformity of voltage output from individual cells.

Overall, the above model simulations have enabled a number of phenomena in the DMFC stack to be related to several performance factors. The modelling tools can be used to provide theoretical explanations to support various experimental observations concerning performance enhancement, thermal inertia etc.

CONCLUSIONS

The current effort in developing a multi cell large-scale stack has shown promising results in terms of electrical performance. In addition, the engineering issues arising from cell scale up and stacking were identified and cost effective solutions were found. The delivered hardware has a total active area of 6800 cm^2, and with currently reported power densities for the MEAs of 100 $mW\,cm^{-2}$ (at 90°C with 1.0 M methanol solution) can deliver in excess of 0.6 kW of electrical energy.

An additional output from this research is that a critical approach towards membrane electrode assembly fabrication is deemed essential as technology is rapidly moving. Currently, hydrogen PEM cells use electrodes that have the catalyst directly deposited on the solid polymer electrolyte, thus achieving a high catalyst utilization. In addition, tailor made membrane electrode assemblies which are designed according to the customer needs and, in addition, the necessary gaskets that are part of the assembly are available from Gore (Primea series), ETEK (ELAT) and DAIS. Ready-made uncatalysed gas diffusion electrodes, like ELAT from ETEK, were evaluated in small cells testing and showed highly promising behaviour. Either of these two solutions can also be adopted in the current stack configuration. Since methanol crossover is still a major concern, especially in the cells with large active area, new low cost solid polymer electrolytes specially designed for DMFC cells can significantly affect the achieved power output.

REFERENCES

1. Troughton, G. L. and Hamnett, A., 1991, *Bull Electrochem*, 7: 488.
2. Prater, K. B., 1994, *J Power Sources*, 51: 129.
3. Scott, K., Taama, W. M. and Cruickshank, J., 1997, *J Power Sources*, 65: 159.
4. Wainwright, J. S., Weng, J. T., Savinell, R. F. and Litt, M., 1995, *J Electrochem Soc*, 142: L121.
5. *Direct Methanol Fuel Cell Review Meeting, Dept of Energy and Advanced Research Projects Agency, Baltimore, April 26–27, 1994*, Executive Summary.
6. Ravikumar, M. K. and Shukla, A. K., 1996, *J Electrochem Soc*, 143: 2601.
7. Surampudi, S., Narayanan, S. R., Vamos, E., Frank, H., Halpert, G., LaConti, A., Kosek, J., SuryaPakash, G. K. and Olah, G. A., 1994, *J Power Sources*, 47: 377.
8. Valdez, T. I., Narayanan, S. R., Frank, H. and Chun, W., 1997, *Proc 12th Annual Battery Conf Applications and Advances* 239.
9. Narayanan, S. R. et al., 1996, *Proc Power Sources Conf, Cherry Hill NJ, USA*.
10. Hogarth, M., Christensen, P., Hamnett, A. and Shukla, A. K., 1995, *J Power Sources*, 55: 87.
11. Scott, K., Taama, W. M. and Argyropoulos, P., 1999, *J App Electrochem*, 28(12): 1389–1397.
12. Argyropoulos, P., Scott, P. K. and Taama, W. M., 1999, *J App Electrochem*, 29: 661–669.
13. Argyropoulos, P., Scott, P. K. and Taama, W. M., 1999, *Electrochimica Acta*, 44: 3575–3584.
14. Argyropoulos, P., Scott, P. K. and Taama, W. M., 1999, Accepted for publication in *Chem Eng J*.
15. Argyropoulos, P., Scott, P. K. and Taama, W. M., 1999, Part 1. Model development. *Chem Eng J*, 73(3): 217–227.
16. Argyropoulos, P., Scott, P. K. and Taama, W. M., 1999, in *5th Europ Sympo on Electrochemical Engineering. Exeter, UK, IChemE, Symp, Series No 145* pp 21–30.
17. Argyropoulos, P., Scott, P. K. and Taama, W. M., 1999, *Chem Eng J*, 73(3): 229–245.
18. Argyropoulos, P., Scott, P. K. and Taama, W. M., 1999, *J Power Sources*, 79(2): 169–183.
19. Argyropoulos, P., Scott, P. K. and Taama, W. M., 1999, *J Power Sources*, 79(2): 184–198.
20. Argyropoulos, P., Scott, P. K. and Taama, W. M., 1999, Submitted for publication to *J Fluids Eng*.
21. Argyropoulos, P., Scott, P. K. and Taama, W. M., 1999, Submitted for publication to *J App Electrochem*.
22. Argyropoulos, P., 1999, *PhD Thesis* (University of Newcastle upon Tyne, UK).

ACKNOWLEDGEMENTS

The authors would like to acknowledge the following for support of this research:

1. The EPSRC for support of Dr W. M. Taama.
2. The European Commission for a TMR Marie Curie B20 research-training trant to Dr P. Argyropoulos.
3. Johnson Matthey Technology Centre for the loan of catalyst material.

ADDRESS

Correspondence concerning this paper should be addressed to Professor K. Scott, Department of Chemical and Process Engineering, University of Newcastle, Merz Court, Newcastle Upon Tyne NE1 7RU, UK.

The manuscript was received 12 October 1999 and accepted for publication after revision 22 June 2000